European Journal of Pharmaceutical Sciences 214 (2025) 107310

Contents lists available at ScienceDirect

European Journal of Pharmaceutical Sciences

journal homepage: www.elsevier.com/locate/ejps

Formulation and evaluation of poly(jasmine lactone) based micelles for improving the oral permeability of acyclovir

Jyoti Verma [a,1], Fanny Frejborg [a,b,1], Marta Mantegna [c], Vishal Kumar [a,d], Veijo Hukkanen [b], Gøril Eide Flaten [c], Jessica M. Rosenholm [a], Kuldeep K. Bansal [a,d,*]

[a] Pharmaceutical Sciences Laboratory, Department of Natural and Health Sciences, Faculty of Science and Engineering, Åbo Akademi University, 20520 Turku, Finland
[b] Institute of Biomedicine, University of Turku, 20520 Turku, Finland
[c] Department of Pharmacy, UiT The Arctic University of Norway, 9019 Tromsø, Norway
[d] Laboratory of Molecular Science and Engineering, Faculty of Science and Engineering, Åbo Akademi University, 20500 Turku, Finland

ARTICLE INFO

Keywords:
Polymeric micelles
Improved permeability
Oral delivery
Herpes simplex virus
Gastroplus
PVPA
Poly(jasmine lactone)

ABSTRACT

Acyclovir (ACV), an antiviral drug, belongs to the BCS class III drug with intermediate solubility and low permeability. The limited permeability leads to low drug absorption, making it poorly bioavailable. Consequently, to achieve the ACV concentration within the therapeutic range, frequent dosing is required which can lead to several side effects. Thus, increasing the permeability of ACV is critical for enhancing bioavailability, overall therapeutic outcomes and patient compliance. Advanced drug delivery systems (DDS), such as polymeric micelles, can be employed to enhance ACV bioavailability, as they offer distinct advantages. Notably, anionic polymeric micelles based on acid functionalized poly(jasmine lactone) copolymer were employed for the first time to improve ACV solubility and permeability. Micelles with size of approx. 100 nm were able to improve the aqueous solubility of ACV from 1.81 mg to 4.32 mg/mL. The anti-viral assay results reveal that ACV loaded micelles are equally effective in both prophylactic and therapeutic settings towards inhibiting herpes simplex virus type 1 compared to free ACV. The permeability study performed via phospholipid vesicle-based permeation assay (PVPA) indicated an improvement in ACV permeability when loaded in polymeric micelles compared to free ACV. This increase was observed both in absence as well as in the presence of an additional mucus layer. In silico simulations performed on GastroPlus® (GPX) software supported the outcomes of PVPA assay in a simulated human model. The obtained results indicated that negatively charged poly(jasmine lactone) micelles could significantly improve the therapeutic outcome of ACV by improving its solubility and oral permeability.

1. Introduction

Acyclovir (ACV), an antiviral drug, is the preferred drug for the treatment of infections caused by herpes simplex virus (HSV) and varicella zoster virus (Gnann et al., 1983; Nair et al., 2014; Sköldenberg et al., 1984) considering its low cost and generic availability. As per the WHO report published on December 11, 2024, an estimate that 3.8 billion individuals globally under the age of 50 (64 %) are infected with HSV-1 (67 %), while 520 million individuals globally (13 %) aged 15 to 49 are infected with HSV-2. ACV belongs to the category of guanosine analogues, having a reported solubility of 1.62 mg/mL and a log*P* value of −1.56 with a plasma half-life of 3 h (Bruni et al., 2013; Shamshina et al., 2017). However, ACV's position in the Biopharmaceutics Classification System (BCS) is dose dependent, i.e., at 200 mg dose, it is classified as BCS-III, but at 800 mg, it exhibits the qualities of a BCS-IV drug/compound. The limited mucosal permeability (15–30 %) renders low drug absorption in the gastrointestinal tract, limiting its therapeutic efficacy. Owing to the low permeability and short half-life, frequent dosing, i.e., 200 mg five times per day, is required to acquire the appropriate drug concentration (Ates et al., 2016; Yan et al., 2013). Thus, improving bioavailability of acyclovir allows for a lower oral dose to achieve the desired systemic exposure. This reduction in oral dose may decrease the amount of unabsorbed drug remaining in the gastrointestinal tract, potentially reducing local gastric side effects. Consequently, the increased burden of viral infections and the continued dependence on ACV as the primary treatment for HSV encephalitis

* Corresponding author.
E-mail address: kuldeep.bansal@abo.fi (K.K. Bansal).
[1] These authors contributed equally.

https://doi.org/10.1016/j.ejps.2025.107310
Received 6 May 2025; Received in revised form 8 September 2025; Accepted 3 October 2025
Available online 4 October 2025

necessitate the development of improved formulation of ACV.

Over the last decade, several drug delivery systems (DDS) have been studied with the aim of improving mucosal permeation bioavailability of ACV. These including microemulsions, multiple emulsions, inclusion complexes, lipid nanoparticles etc., which were devised to improve mucosal permeation. For instance, Ghosh et al. formulated a micro-emulsion using Labrafac™ as the base, Labrasol® as the surfactant, and Plurol® Oleique as the co-surfactant for the oral administration of ACV. The in vivo investigation in rats demonstrated a 13-fold increase in bioavailability of the microemulsion formulation, compared to the commercially available tablets (Aquivir). The higher absorbance was owing to the presence of surfactant or large surface area of micro-emulsion droplets with better stability in the gastrointestinal tract (Ghosh et al., 2017). However, the high concentration of surfactants can cause severe toxicities.

In another study, ACV loaded bilosomes were prepared by utilizing cholesterol as a lipid. The ex vivo gut permeation study demonstrated a significant improvement in the penetration of ACV loaded bilosomes compared to the ACV solution and the marketed formulation. Further, an in vivo pharmacokinetic study on Wistar rats shows that the ACV loaded bilosomes increased relative bioavailability by 4.3 and 2.5 fold ($p < 0.05$), compared to the ACV solution and the marketed formulation, respectively (Saifi et al., 2020). Nevertheless, poor loading, drug leakage on storage and lipid stability are some concerns associated with this DDS.

Polymeric micelles have emerged as a promising DDS with several benefits compared to carrier systems discussed above. Polymeric micelles, being fabricated from amphiphilic polymers, does not require additional surfactants for stabilization and demonstrate improved stability upon dilution in biological fluids (Kedar et al., 2010; Xie et al., 2024). Further, polymeric micelles offer greater flexibility in accommodating a wider range of drug molecules, including those with larger molecular weights, while also enabling controlled and targeted delivery with stimuli-responsive release (Assiri et al., 2024; Bansal and Lariya, 2018). Together, these features highlight that polymeric micelles are also an attractive carrier system for improving the oral permeation of drugs. Studies have already demonstrated their capability in enhancing the permeability of numerous drug molecules (Salimi et al., 2019; Sze et al., 2019). For instance, Shalimi et al. prepared polymeric micelles loaded with deferoxamine mesylate (DFO) via the film hydration method using carbomer 934, Poloxamer (Pluronic® *P* 407) polymers. It was found that the prepared polymeric micelles with small particle size offered 3 times higher oral permeation of DFO by enhancing the surface area as well as via protecting the drug against degradation from acidic and alkaline conditions (Salimi et al., 2019).

To the best of our knowledge, despite being a well investigated and established carrier system, polymeric micelles have not yet been explored for the improvement of oral permeability of ACV. The likely cause for the exclusion may be attributed to the inadequate loading in the micelle hydrophobic core due to the hydrophilic characteristics of ACV. To overcome this constraint, we have employed negatively charged poly(jasmine lactone) (PJL) based copolymer micelles, which to date have been shown to enhance the water solubility of several hydrophobic drugs (Ali et al., 2022; Bansal et al., 2023a, 2023b). The existence of "ene" groups on the backbone of PJL provides the possibility to synthesize anionic polymer by incorporating carboxylic acid groups in side chain (Bansal et al., 2023b; Rahman et al., 2022). The negatively charged nanocarriers appear to trigger tight junctions (specialized intercellular junction) located primarily in epithelial and endothelial cells, particularly those that line mucosal surfaces such as the intestinal epithelium, blood-brain barrier, and other barrier tissues. It has been reported that carboxymethyl chitosan/chitosan nanoparticles with a negative surface charge caused a greater disruption of tight junctions and improved the movement of substances between cells compared to similar nanoparticles with a positive surface charge (Spleis et al., 2023). Researchers discovered that negatively charged silica nanoparticles can attach to epithelial cells and temporarily open tight junctions (Lamson et al., 2020). Another work by Yu et al. showed that anionic SLNs were better at uptake through the lymphatic pathway than positively charged particles (Yu et al., 2019). The strength of intestinal tight junctions is crucial for controlling passage through the intestinal lining, helping to protect against harmful substances, infections, and toxins. When tight junctions are damaged or opened, it increases intestinal permeability, often called “leaky gut,” allowing harmful substances like bacteria, undigested food, and toxins to enter the bloodstream (Lee et al., 2018). Thus, in the current study, we developed polymeric micelles via modified nanoprecipitation method to encapsulate ACV by utilizing acid functionalized PJL based amphiphilic co-polymers, i.e. mPEG-b-PJL-COOH and homopolymer B-PJL-COOH. Further, we evaluated this system for permeability enhancement, drug release, in vitro anti-viral activity on HSV-1, as well as examined oral absorption profile in-silico using GastroPlus$^{(R)}$ and compared the results with free ACV.

2. Materials and methods

1,5,7-triazabicyclo[4.4.0]dec-5-ene (TBD) (98 %), mercaptopropionic acid (99 %), dimethoxy-2-phenylacetophenone (99 %), deuterated dimethyl sulfoxide (DMSO-d6), $CDCl_3$, THF, DMF, DCM, HPLC grade methanol (≥99.9 %), acetone (≥99.8), ethanol (96 %, v/v), calcein, mucin from porcine stomach type III (bound sialic acid 0.5–1.5 %, partially purified), potassium phosphate monobasic, sodium chloride, sodium hydroxide, sodium phosphate dibasic dodecahydrate, hydrochloric acid (HCl) and ether were purchased from Sigma-Aldrich. Jasmine lactone (≥97 %) was purchased from Lluch Essence (Barcelona, Spain). Acyclovir (>99 %) and resazurin were purchased from TCI Europe Pvt. Ltd. Titriplex® III was purchased from Merck KGaA, while HPLC grade acetonitrile was purchased from VWR International. Trifluoroacetic acid, reagent grade, 99 %, was obtained from Honeywell. Lipoid egg phospholipids E-PC (egg phosphatidylcholine, 80 % phosphatidylcholine) was purchased from Lipoid (Ludwigshafen, Germany), while plates and filter inserts (transwell, $d = 6.5$ mm) were purchased from Corning Inc. The mixed cellulose ester filters (0.65 um pore size) and Whatman® nucleopore track-etch membrane filters (0.4 and 0.8 μm pore size) were obtained from Millipore and Whatman respectively. Milli-Q water was used for formulation preparation (Milli-Q Synthesis, Millipore). The 0.45 μm cellulose acetate membrane filter was purchased from VWR.

2.1. Synthesis and characterization mPEG-b-PJL-COOH and b-PJL-COOH

The synthesis of $mPEG_{5k}$-b-PJL-COOH is reported in our previous publication and the same polymer has been used in this study (Molecular weight - 11.4 kDa, with 24 –COOH groups, and CMC of 10.2 ± 3.9 μg/mL(Ali et al., 2022; Bansal et al., 2021)(Ali et al., 2022; Bansal et al., 2021). For the synthesis of carboxylic functionalized homopolymer poly (jasmine lactone) (B-PJL-COOH), the parent homopolymer benzyl-PJL (B-PJL) was first synthesized by ring opening polymerization, and then the thiol-ene click reaction was utilized to insert -COOH groups. In brief, the dried jasmine lactone (10 g, 59 mmol) was weighed in an RBF and then dried benzyl alcohol (0.41 mL, 3.96 mmol) as an initiator was added to it and stirred to make a homogeneous mixture. Next, dried TBD (0.16 g, 1.18 mmol) as a catalyst was added to the above RBF and reaction was continued at room temperature overnight in a nitrogen environment. For reaction quenching, benzoic acid (0.28 g, 2.36 mmol) dissolved in acetone was added to the RBF and stirred for 30 min and the resultant solution was precipitated twice in ice cold methanol. The residual solvent was removed under vacuum, and the obtained pure polymer (6.0 g) was characterized by ^{1}HNMR. For functionalization, (1 g, 0.40 mmol) of B-PJL and (0.2 g, 1.1 mmol) of DMPA (photocatalyst) were dissolved in 5 mL of THF and added to RBF containing (1.8 g, 17.5 mmol) of 3-mercaptopropionic acid, stirred in a UV cabinet fitted with a

blacklight 368 nm lamp (15 W, Sylvania). The progress of the reaction was monitored by HNMR, which showed a 100 % conversion after 4 h. The THF was evaporated, and reaction mixture was precipitated in ice-cold diethyl ether (X2), followed by the removal of residual solvent under vacuum to afford 0.92 g of the pure (B-PJL-COOH) polymer.

The chemical structure and molar mass (Mn) of synthesized polymers were analysed by ^{1}HNMR. Deuterated chloroform (CDCl3) and deuterated acetone (Acetone-d6) were used as solvents for NMR.

The number-average molar mass (Mn), weight-average molar mass (Mw), and mass distribution (polydispersity (Đ), Mw/Mn) of the synthesised polymer were also determined by size exclusion chromatography (SEC). A 2 mg/ml solution of polymer in THF was used to be analysed by the instrument fitted with a low-temperature evaporative light scattering detector (LT-ELSD) with an AM GEL linear column (10 μm particle size) and an AM gel guard column (300 × 7.8 mm). Column calibration was done using a narrow polystyrene standard of known Mn and Đ in the range of 600–2300 kDa. Tetrahydrofuran (THF) was used as the mobile phase at 40 °C with a flow rate of 1 mL/min.

^{1}HNMR details of B-PJL: (500 MHz, $CDCl_3$) δ 7.35 (m, 5H), 5.5 (m, 13H), 5.3 (m, 13H), 5.1 (s, 2H), 4.9 (m, 13H), 4.02 (m, 1H), 3.61 (s, 1H), 2.28 (m, 56H), 2.03 (m, 29H), 1.58 (m, 58H), 0.98 (m, 42H).

^{1}HNMR details of B-PJL-COOH: (500 MHz, $(CD_3)_2CO$) δ 7.35 (m, 5H), 4.9–5.3 (m, 15H), 3.61 (s, 2H), 2.7 (m, 27H), 2.58 (m, 44H), 1.5–1.9 (m, 146H), 0.98 (m, 42H).

2.2. Polymeric micelles preparation and characterization

The polymeric micelles were prepared by following nano-precipitation method with slight modifications (Pyrhönen et al., 2022). Briefly, ACV (5 mg) was dissolved in 0.1 N HCl solution (1 mL) to make aqueous phase. The mPEG-b-PJL-COOH (16 mg), and B-PJL-COOH (4 mg) were dissolved in acetone (1 mL) with the aid of vortex. This organic mixture was added dropwise into aqueous phase under stirring and then the pH of the solution was raised to pH 5 (equivalent to blank polymer solution pH) using 0.1 M NaOH solution. After pH adjustment, the solution was left stirred for at least 12 h at room temperature to ensure the complete removal of the organic solvent (acetone). To separate the unentrapped drug, the prepared micelles (further referred as B-COOH micelles) were centrifuged (Microcentrifuge, Scanspeed, Labogene, Lynge, Denmark) for 10 min at 13,500 RPM. The supernatant was then filtered through a 0.45 μm cellulose acetate membrane, syringe filter. A similar method was utilized to prepare ACV micelles with mPEG-b-PJL-COOH (20 mg) polymer alone (without B-PJL-COOH). The blank micelles were prepared with similar methods without using ACV.

The drug content was determined using UV–Vis spectrophotometer (NanoDrop 2000c spectrophotometer from Thermo Fisher Scientific) after appropriate dilutions in methanol at λ_{max} – 252 nm. The size and polydispersity index (PdI) of the polymeric micelles were obtained on ZetaSizer Nano-ZS (Malvern Instruments, UK) at 25 °C with an equilibration time of 60 s. Samples were placed into the appropriate cuvettes for analysis after being diluted (100 times) with Milli-Q water. The dispersion medium was Milli-Q water with a refractive index of 1.33, and the particle refractive index value used was 1.59 for all the DLS measurements.

For the calculation of entrapment efficiency (EE), the calculated amount of micelles were diluted in water and drug content was then quantified using a UV spectrophotometer. The percentage of EE was calculated using the given formula (Bansal et al., 2018).

$$EE(\%) = [\text{Weight of loaded drug} / \text{Weight of drug in feed}] * 100$$

Further, transmission electron microscopy (TEM) was employed to confirm the particle size and to ascertain the shape. TEM grids stained with uranyl acetate (negative) were imaged on a JEM 1400-Plus instrument (JEOL Ltd., Tokyo, Japan). The micelles formulation was diluted with water (50 μg/mL relative to polymer concentration) and then passed through a membrane syringe filter (0.45 μm) before placing on TEM grid. The zeta potential of the micelles was determined on Malvern Zetasizer Nano-ZS. After rinsing the folded capillary cell (DTS1070), it was filled with the sample solution, previously diluted with 25 mM HEPES buffer (100 μg/mL relative to polymer). Measurements were performed at 25 °C with an equilibration time of 120 s.

Three independently prepared samples were used for each micelles sample, and each sample was measured three times using the Zetasizer.

2.3. Stability study

To conduct the stability study of prepared ACV loaded micelles, the filtered samples were kept at room temperature (25 ± 2 °C) for 6 months. Initially on day 0 and after six months, samples were examined visually for changes in appearance and precipitation. Samples were further analyzed by DLS and HPLC, to observe the change in size and drug content (filtered samples for drug content to remove any precipitated drug), respectively.

HPLC condition: The mobile phase is composed of milli-Q water with 0.1 % formic acid (mobile phase A) and acetonitrile (mobile phase B). In a grading setting, the conditions for mobile phase B were 10 % v/v for 0 min, 15 % v/v for 2 min, 20 % v/v for 4 min, 30 % v/v for 6 min, and 10 % v/v for 8 min. The flow rate was 1 mL/min, and the volume injected was 10 μL using an autoinjector. The analytes were detected using UV detection at 254 nm using an ODS-3, C18 (250 × 4.6 mm i.d., 5 μ) column for separation.

2.4. Drug release

The release profile of free ACV and ACV in micelles were evaluated using a dialysis method at 37 °C (Bansal et al., 2018). A calculated amount of ACV loaded polymeric micelles/ACV solution equivalent to 1 mg/mL of ACV concentration were placed in dialysis membrane (Spectra/Por) having the molecular weight cut-off (mwco) of 6–8 kDa. The samples were then dialyzed against 40 mL of fasted state simulated gastric fluid (Biorelevant FaSSGF, pH 1.2), at 37 °C for 2 h and then the release was continued by changing the release media from FaSSGF to fasted state simulated intestinal fluid (Biorelevant FaSSIF, pH 6.8) to mimic oral delivery. Samples (1 mL) were withdrawn directly from the dialysis medium (after shaking) at predetermined time intervals and replaced with equal volume of fresh media. The samples were then analyzed with UV–Vis spectrophotometer to calculate the cumulative amount of ACV released from the dialysis bag.

2.5. Partition co-efficient determination (Po/w)

The partition coefficient of ACV and ACV micelles was determined via n-octanol/water system using shake flask method. 5 mg of ACV was dissolved in 4 mL of milli-Q water, and the drug solution was transferred into a separating funnel. Next, 4 mL of n-octanol was added into the separating funnel and funnel was vigorously shaken for at least 5 min to combine the two phases and then placed still to separate the two phases. On the subsequent day, both phases were collected separately into vials, and after appropriate dilutions, the samples were analysed on a UV–Vis spectrophotometer to ascertain the amount of ACV in each phase. In place of drug solution, the micelles solution was used to determine the Po/w of ACV micelles. Then, the log Po/w was calculated using the formula: *P*ow=Xo/Xw, where Xo is fraction of drug in oil phase (organic phase) and Xw is fraction of drug in aqueous phase.

2.6. Antiviral studies

2.6.1. Cells and viruses

U373MG cells (here referred to as MG), currently reclassified as U251 (glioblastoma, HTB7, ATCC), representing neuronal cells, were used for antiviral and cytotoxicity assays, and were maintained in Dulbecco's modified eagle medium (DMEM; Gibco, Thermo Fischer

Scientific) supplemented with 7 % fetal bovine serum (FBS; Gibco, Thermo Fischer Scientific), 10 μM GlutaMax (Gibco) and 10 μg/mL gentamycin. Vero cells (African green monkey kidney cells, CCL-8, ATCC) were used for viral titrations and plaque reduction assays, and were maintained in DMEM supplemented with 7 % FBS, 10 μM GlutaMax and 10 μg/mL gentamycin.

HSV-1 (17+) Lox_{PmCMV}GFP (abbreviated as HSV-1-GFP) was used for the antiviral and plaque reduction assays (Snijder et al., 2012). The virus was propagated and stored in 9 % milk as previously described (Kalke et al., 2022).

2.6.2. Antiviral assay

Subconfluent MG cells in 96 well plates were treated with 1 μg/mL of free ACV, ACV in micelles or corresponding blank micelles, either prophylactically or therapeutically, directly administered to the cell medium. The prophylactic treatment was administered 24 h pre infection, and the therapeutic treatment was administered 1 h after infection and half of the parallels were washed 3 h after treatment. The timeline is illustrated in Scheme 1. The cells were washed prior to infection and infected with 20 plaque forming units (pfu) per well with HSV-1-GFP in DMEM supplemented with 2 % FBS and gentamycin. The infection medium was washed 1 h after infection, with medium replaced to DMEM supplemented with 7 % FBS 10 μM GlutaMax and gentamycin. The supernatant was collected 48 h post infection for quantification.

The viral titer in the supernatant was quantified using plaque titration. Briefly, the supernatant was titered on confluent Vero cells in 96 well plates and then overlaid with DMEM 7 % FBS containing 80 mg/mL (40 mg/mL after addition) human immunoglobulin G (HyQvia) after 1.5 h. After 72 h the cells were fixed with methanol and stained with 0.5 % crystal violet, and plaques were counted and quantified.

2.6.3. Plaque reduction assay

Confluent Vero cells in 96 well plates were infected with 20 pfu/well of LoxGFP in DMEM 2 % FBS and 1 h after infection, 1 μg/mL of free ACV, ACV in micelles or blank micelles were administered to the medium. 3 h after treatment, 80 mg/mL (40 mg/mL after addition) IgG was added to the medium. 48 h after infection, the cells were fixed with methanol and stained with 0.5 % crystal violet, plaques were counted and quantified.

2.7. In vitro permeability study

2.7.1. Preparation of the PVPA barriers

The egg phosphatidylcholine (E-PC) liposomes used for the phospholipid vesicle-based permeation assay (PVPA) barriers were obtained from film hydration method, as previously described (Naderkhani et al., 2015). Briefly, E-PC was dissolved in a mixture of chloroform and methanol (2:1 v/v), and the organic solvents were later completely removed on a rotary evaporator under a vacuum of 55 hPa at 45 °C for a period of 3 h. The resulting lipid film was hydrated with phosphate buffer (pH 7.4) and ethanol (10 % v/v) in order to obtain a 6 % (w/v) liposomal dispersion. Two different size distributions were reached through hand extrusion by using filters with different pore sizes (0.4 μm and 0.8 μm).

The PVPA barriers were then prepared by forcing the two liposome dispersions of 0.4 um and 0.8 μm into the pores and on top of a cellulose ester filter by centrifugation, followed by a freeze-thaw cycle. The barriers were stored at −80 °C for at least 1 h before use and then heated at 65 °C for 30 min before starting the experiment (Falavigna et al., 2018; Flaten et al., 2006).

2.7.2. Mucus barrier

To mimic the small intestine mucus layer, mucin from porcine stomach type III (10 mg/mL) was hydrated with PBS (pH 7.4), according to the reported method (Falavigna et al., 2018). The suspension was then added on top of the barrier before the addition of the test formulation in the donor compartment, while being careful not to disrupt the mucin layer.

2.7.3. Permeability assay

The permeability assay of ACV was performed based on the previously reported methods (Falavigna et al., 2018; Flaten et al., 2006). The experiments were performed at room temperature in the absence and presence (adding 50 μL of hydrated mucin on top of the barrier) of mucin and 100 μL of the drug solution (1 mg/mL) or formulation was added into the donor compartment, while 600 μL of PBS (pH 7.4) were added in the acceptor wells. To maintain sink conditions, the barriers were moved at certain time intervals to a new acceptor compartment filled with fresh PBS. The electrical resistance was measured at the end of the experiment to confirm the integrity of the barriers. The experiment was performed at least in triplicates, and the apparent permeability coefficient was calculated from Fick's Law for steady-state conditions:

$$P_{app}\left(\frac{cm}{s}\right) = \frac{\Delta Q}{\Delta t} x \frac{1}{AC_d}$$

Where ΔQ/dt is the slope at the steady-state conditions (nmol/s), A represents the surface area of the PVPA barriers (cm^2), and C_d is the concentration of the compound in the donor compartment (nmol/mL).

To understand the effect of the formulation on the barrier and its integrity, the permeability of a hydrophilic marker in micelles was tested during the study and was quantified spectrofluorometrically on the Spark® plate reader (Tecan Trading AG, Switzerland), as described in a previous paper (Falavigna et al., 2019).

2.7.4. Quantification of ACV

ACV was quantified on an Acquity UPLC-PDA class H (Waters Corporation, Milford, USA) equipped with a C_{18} column (1.7 μm, 2.1 × 100 mm; Waters Corporation, Milford, USA). ACV was detected at a wavelength of 253 nm for UV detection, and the total measuring time was 6 min. The flow rate and the column temperature were set to 0.6 mL/min and 60 °C, respectively. The mobile phases consisted of 0.1 % TFA in Milli-Q water (mobile phase A) and 0.1 % TFA in acetonitrile (mobile phase B), with isocratic conditions (0.5 %, v/v, mobile phase B) for 2 min, followed by a gradient elution cycle (0.5–30 % v/v, mobile phase B) of 4 min. The sample concentration was determined from a standard curve by diluting known amounts of ACV in water. The calibration curve resulted in good linearity in the 1–20 μg/mL concentration range with an R^2 of 0.9992. To exclude interference because of similar retention time, separate measurements for the blank micelles were performed. All measurements were carried out in triplicates.

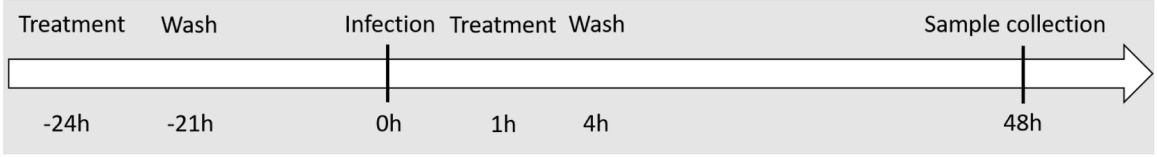

Scheme 1. Timeline of the antiviral assay.

2.8. Cytotoxicity study

2.8.1. Cell growth media

MDA-MB-231, driven from human breast adenocarcinoma cells were cultured in high glucose DMEM, which was supplemented with 10 % FBS, 2 mM L-glutamine, and 1 % penicillin-streptomycin (v/v) at 37 °C with 5 % CO_2, whereas MG cells were cultured on same media as discussed in antiviral section (2.6.1).

2.8.2. Cytotoxicity assay

The assessment of the cytotoxicity of blank polymeric micelles were performed using the MTT assay on MDA-MB-231 and MG cells using the previously reported procedure with minor modifications (Shakri et al., 2025). Briefly, 100 μL of cell suspension, diluted up to the concentration of 5,0000 cells/mL, was seeded into a 96-well plate and incubated for 24 h. Later, mPEG-b-PJL-COOH and B-COOH (without drug) micelles were diluted to make 250, 500 and 750 ug/mL in prewarmed (37 °C) growth media. The cell culture media in a 96-well plate was replaced with micelles samples after 24 h incubation and further incubated for 48 h at 37 °C, 5 % CO_2. After 48 h incubation, 10 μL of MTT solution (5 mg/mL in PBS) was added to each well and incubated for 3 h. The resulting formazan crystals were dissolved using 100 μL of DMSO, and absorbance was measured at 570 nm using a microplate reader. The percentage of cell proliferation was than calculated compared to untreated cells (100 % viability).

3. GastroPlus-based simulation and prediction studies

The GastroPlus program (version 10.1, Simulation Plus, Inc., Lancaster, USA) offers a range of drug delivery route selections and in this investigation, we have chosen the oral route. The input parameters can be classified into three main tabs: (a) compound tab (describing the physicochemical properties of ACV) for entering necessary information related to the drug; (b) formulation tab (including experimental values such as solubility, particle size, and permeation coefficients); and (c) physiological tab (for predicting and simulating conditions). The experiment performed a prediction analysis using a human model with a simulation duration of 24 h. For each simulation and prediction run, we employed experimental, theoretical (literature based), and default values for the input settings (Kasif et al., 2024). Utilizing values from Table 1, which contained drug-related information (including experimental, literature, and default values), the algorithm estimated the time course of plasma drug concentration in human weighing 70 kg given 100 mg dose of ACV (solution) and ACV in form of micelles over the time course of 24 h.

Table 1
Input parameters in the GastroPlus® software.

S. no.	Parameters	Values	
		Pure ACV	**ACV in Micelles**
1	Molecular formula	$C_8H_{11}N_5O_3$	$C_8H_{11}N_5O_3$
2	Molecular weight	225.21	225.21
3	Density (g/mL)	1.20	1.20
4	Pka	2.27, 9.25	2.27, 9.25
5	Log P	−1.60	−0.91
6	Melting point	256.60	256.60
7	Dose (mg)	100	100
8	Body weight (kg)	70	70
9	Mean precipitation time (s)	900	900
10	pH for reference solubility	5	5
11	Diff. coefficient ($cm^{2/s} * 10^5$)	0.97	0.97
12	Blood/plasma conc. Ratio	1.07	1.07
13	CL(l/h)	24.03	24.03
14	Vc (L/kg)	0.87	0.87
15	Simulation time (h)	24	24
16	Permeability (PVPA)	0.00	0.050
17	Solubility	1.81 mg/mL	4.32 mg/mL
18	Particle size (nm)	1*	100
19	Solubilizer	-	Yes
20	Solubilizer (Molecular Weight)	-	7500

* The particle size of pure ACV in solution was considered as 1 nm, as it exists in a molecularly dissolved state.

4. Statistical analysis

All values were expressed as the mean ± standard error of the mean (mean ± SEM) of three independent experiments except for antiviral assays, with two independent experiments and five parallels, and permeability assay with six independent experiments. The data for multiple treatment groups were analyzed using one-way ANOVA (Multiple Comparisons) followed by Tukey's multiple comparisons test, computed using GraphPad Prism (Version 5.02) software, if not stated distinctly. Differences were considered as statistically significant at $P < 0.05$, when compared with controls.

5. Results and discussion

5.1. Synthesis and characterization of parent and carboxyl-functionalizedpoly(jasmine lactone)

The schematic representation for the synthesis of the polymers is given in Scheme 2. The conversion of monomer to polymer was monitored by ^{1}H NMR and after purification (88 % conversion), the molar mass of pure polymer was calculated by interpreting and comparing the proton of the initiator at 5.2 ppm and the proton of PJL at 4.9 ppm with respect to the proton of the methylene group of PJL at 0.98 ppm (Fig. 1). Fourteen repeating unit of jasmine lactone was attached to benzyl alcohol, which suggest the molecular weight of 2.4 kDa.

Next, the purified B-PJL was converted into carboxyl-functionalized poly(jasmine lactone) (B-PJL-COOH) (Scheme 2–2), by stirring the reaction mixture for 4 h under UV light. The ^{1}H NMR spectra (Fig. 2) showed complete disappearance of the peak at 5.5 ppm, suggesting 100 % consumption of the double bond by thiol groups. The molecular weight of polymer after purification was calculated by interpreting and comparing the proton of benzene ring at 7.3 ppm and the proton of PJL and CH_2 of benzyl alcohol at 4.9 to 5.2 ppm with respect to the protons of 3-mercaptopropionic acid at 2.7 ppm. The calculated molecular weight based on 100 % conversion obtained through ^{1}HNMR was found to be 3.9 kDa. The homopolymer B-PJL-COOH is insoluble in water, while the water solubility of block copolymer mPEG-b-PJL-COOH is approximately 2 mg/mL.

Furthermore, to confirm the molecular weight and mass distribution, size exclusion chromatography (SEC) analysis (Figure- 3A) was performed, and the results are presented in Table 2.

5.2. Preparation and characterization of polymeric micelles

Following our previous study, the PJL based polymeric micelles were prepared with the aid of a COOH functionalized, mixture of mPEG-b-PJL-COOH and B-PJL-COOH polymers as well as with mPEG-b-PJL-COOH alone through a modified nanoprecipitation method, as the ACV is poorly soluble in acetone/methanol and freely soluble in HCl (50 mg/mL in 1 N HCl solution). Later, micelles were purified by centrifugation, followed by filtration to remove the unentrapped drug. The purified micelles were then characterized for their drug content and size after appropriate dilutions. To determine whether the UV method is efficient in determining the ACV content in the micelles, we did some control measurements. The stock solution of ACV in water was diluted with water (10 μg/mL), blank micelles in water (equivalent to 10 μg/mL for ACV), and ACV micelles in water (diluted to up to the extent to get absorbance below 1), after which the absorbance was measured at 252 nm. As shown in Fig. 3B, there was some absorbance at 252 nm from the blank polymer, so we used the blank polymer micelles solution as blank, while estimation through UV spectrophotometer, indicating the

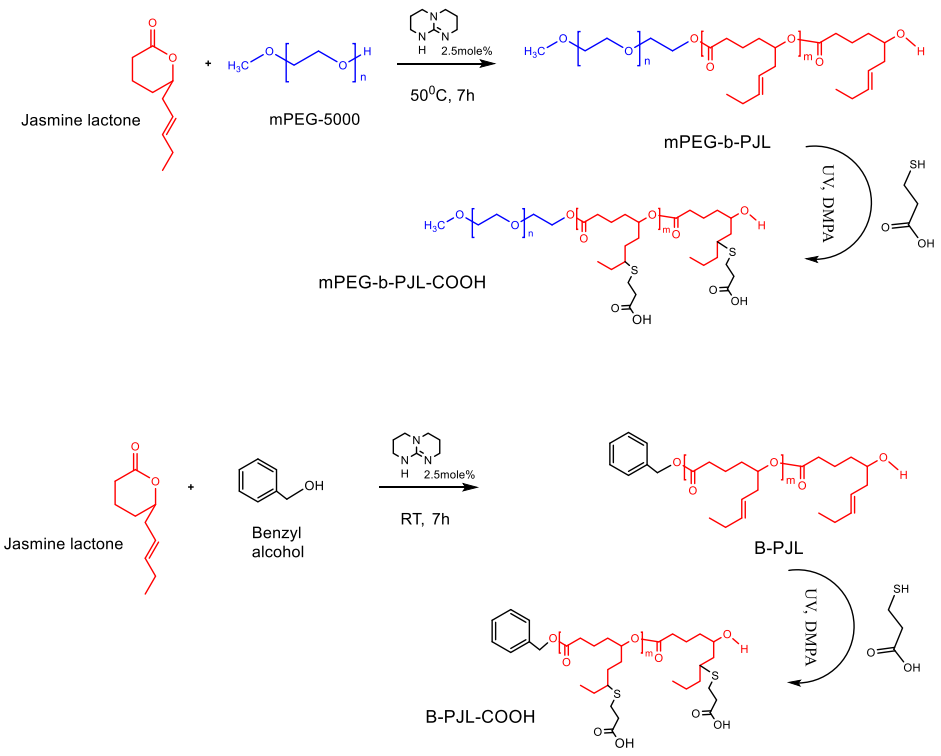

Scheme 2. (1) Synthesis of block copolymer mPEG-b-PJL and post synthesis functionalization to introduce COOH functional group; (2) synthesis of B-PJL-COOH homopolymer.

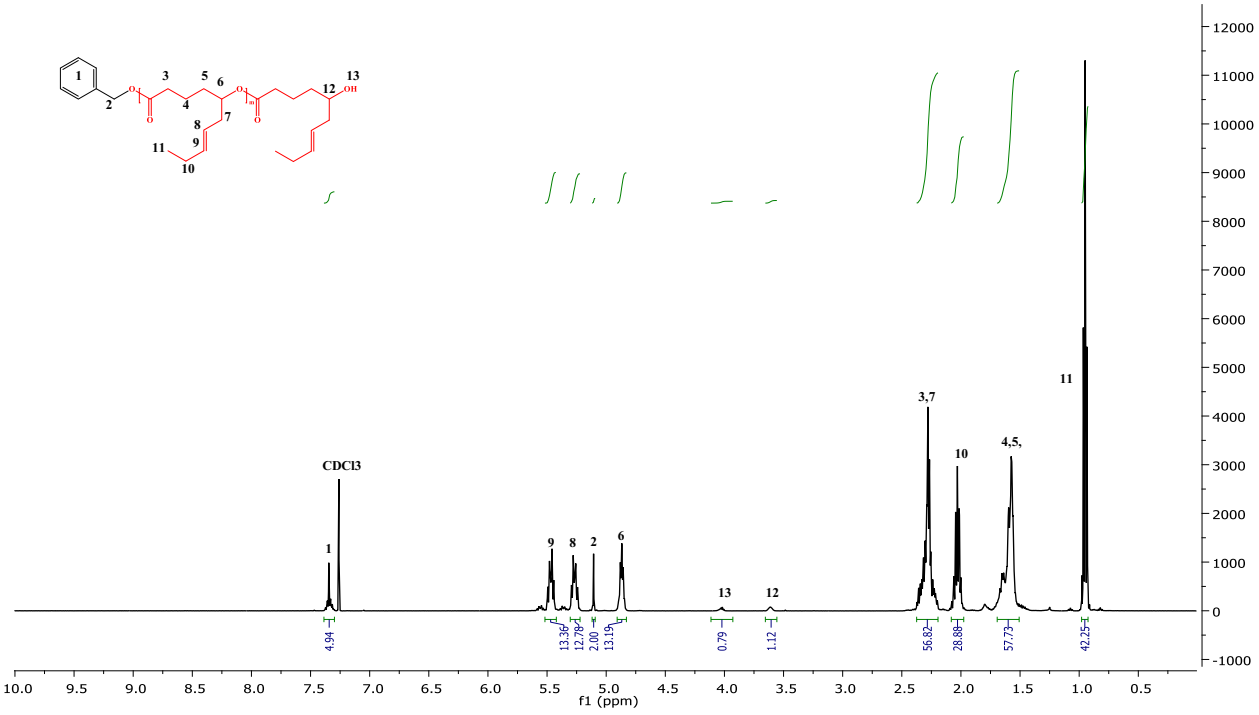

Fig. 1. ^{1}H NMR spectra of synthesized parent homo polymer (B-PJL) in $CDCl_3$.

adequacy of UV method to reveal ACV content estimation through UV spectrophotometer.

The drug content of ACV micelles prepared with mPEG-b-PJL-COOH alone was found to be 1.90±0.01 mg/mL with drug encapsulation efficiency (EE) of 42.22 % and the micelles prepared with the combination of polymers (B-COOH) was 4.32±0.05 mg/mL having EE of 86.40 %. We observed that the micelles prepared using combining two polymers performed better in terms of drug loading compared to mPEG-b-PJL-COOH based micelles alone. Therefore, all further studies were performed using B-COOH micelles (referred to as ACV micelles). The water solubility of free ACV was found to be 1.81±0.12 mg/mL via the similar modified nanoprecipitation method without the aid of polymers

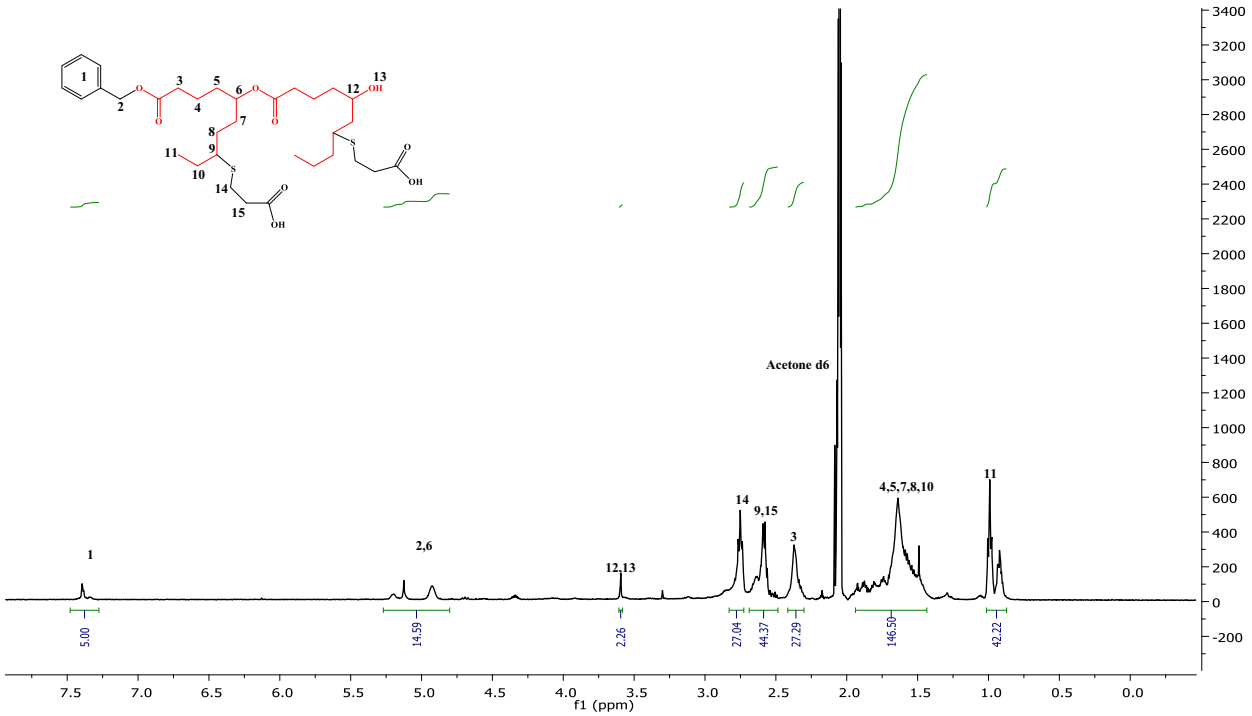

Fig. 2. ^{1}H NMR spectra of synthesized B-PJL-COOH in deuterated acetone-d6.

Table 2
Molecular weight of synthesized polymers assessed by NMR and SEC.

SN	Polymer	Mn by ^{1}H NMR [kDa]	Mn by SEC [kDa]	Đ (M_w/M_n)
1	mPEG-b-PJL*	9.03	8.80	1.40
2	mPEG-b-PJL-COOH*	11.45	9.40	1.40
3	B-PJL	2.46	2.65	1.52
4	B-PJL-COOH	3.93	3.85	1.38

* These previously published results (Bansal et al., 2021) have been included here for reference.

indicates that micelles increased the aqueous solubility of ACV by approximately 2.4-fold. Further, the size and shape were confirmed using TEM imaging of ACV micelles with uranyl acetate negative staining at room temperature, indicating a spherical shape with average size of around 100 nm (Fig. 4A).

5.3. Stability study of ACV micelles

In this study, we interpreted micellar stability in terms of kinetic stability. Kinetic stability refers to the long-term behavior of the system and provides information on the pace at which polymer exchange and micelle destruction occur. Consequently, the stability of ACV micelles at room temperature (25 ± 2 °C) for a duration of 6 months was assessed. No evidence of visible changes such as precipitation in the micellar solutions were observed after 6 months of storage. To detect the change in drug content, zeta potential, hydrodynamic size and PdI, the micelles were analyzed with HPLC and DLS. The HPLC was utilized to determine the stability of the drug, as UV spectroscopy might unable to detect any degradable moieties. The chromatograms of free ACV and ACV micelles at month 0 and at month 6 is presented in Fig. 4B (Retention time (RT)-2.1 min), and an additional peak was observed at month 6 for micelles at RT- 1.4 min, indicating only minor degradation of drug, suggesting good stability of ACV within micelles for up to 6 months.

The micelles showed 4.66 % increment in the Z-average size and 45.29 % increment in PdI, as well as a reduction of 36.19 % in zeta

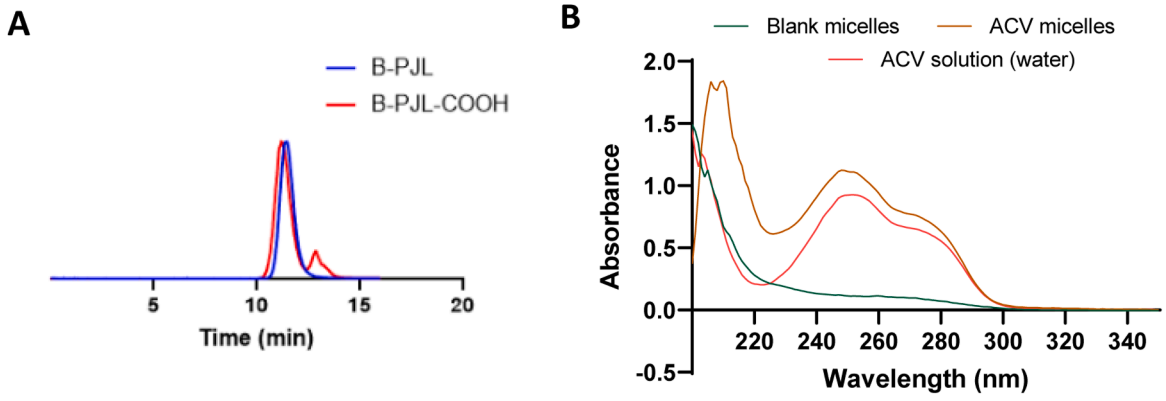

Fig. 3. (A) Overlapped SEC chromatogram (normalized) of the synthesized parent homopolymer (B-PJL) and carboxylic functionalized homopolymer (B-PJL-COOH). The small peak at 13 min corresponds to THF. (B) UV spectra of ACV solution, ACV micelles and blank micelles in water.

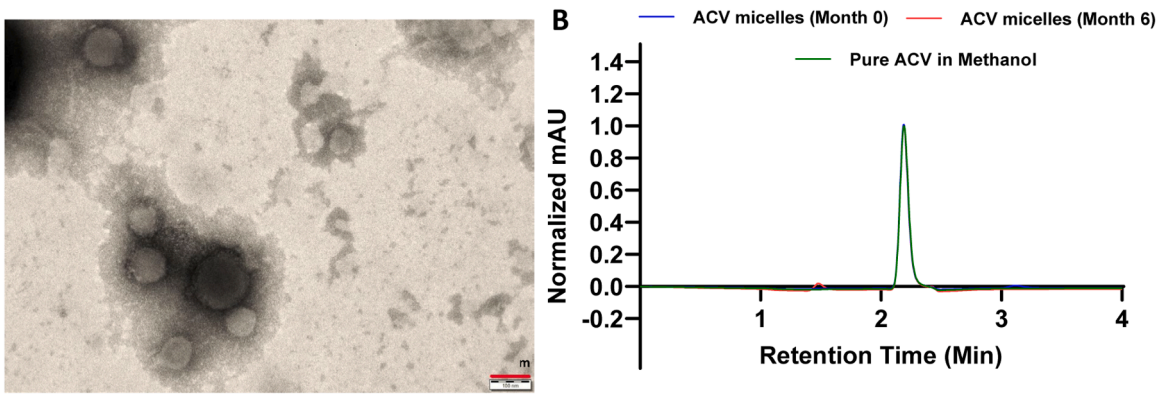

Fig. 4. (A) TEM image of ACV micelles after uranyl acetate negative staining (Scale 100nm); (B) HPLC chromatogram of pure ACV in methanol, ACV loaded micelles on day 0 and after 6 months storage at room temperature.

potential (Fig. 5A&B, Table 3). A substantial change in the PdI could be attributed to the additional peak observed in the size distribution graph, which indicates some aggregation of micelles, but the mean size was still close to 100 nm. The zeta potential of ACV-loaded micelles is relatively low (−12.10 ± 1.65 mV), which might suggest limited effect on stability from electrostatic repulsion between the micelles. However, their stability is mainly due to steric stabilization from the PEG corona rather than electrostatic mechanisms. The blank micelles have zeta potential in similar range (−15.06 ± 9.64 mV), which suggests that ACV loading does not affect the surface charge. Despite the lower charge, the micelles remain stable due to a combination of steric hindrance, core–shell architecture, and polymer–drug interactions (Cabral and Kataoka, 2014).

Table 3
Drug content, Z-average size, and PdI of freshly prepared ACV loaded micelles (0 months) and after 6 months of storage at room temperature (25 °C) measured in deionized water.

Samples	ACV content in mg/mL (±SD)	Z-average size in nm (±SD)	PdI (±SD)	Zeta Potential (mV)
ACV micelles (0 months)	4.32±0.05	103±2	0.19 ±0.01	−12±2
ACV micelles (6 months)	4.07±0.35	108±18	0.34 ±0.04	−8 ± 1
% Change from 0 month to 6 months	(-) 4.06 %	4.66 %	45.29 %	36.19 %

5.4. *In vitro release study*

For any nanotechnology-based formulation, it is important that the encapsulated drug will release at a sufficient rate to produce a pharmacological response. Thus, to assess the release pattern of ACV from the ACV micelles, we performed experiments initially in fasted state simulated gastric fluid (Biorelevant FaSSGF, pH 1.2) for 2 h and continue in fasted state simulated intestinal fluid (Biorelevant FaSSIF, pH 6.8) up to 24 h to mimic the GIT conditions. A fast release pattern of ACV was observed from the control as well as from the micelles within 6 h, where >80 % of ACV was released (Fig. 6A). The ACV micelles exhibit 100±1.76 % release within 24 h, while the free ACV sample releases 88.68±2.09 %. The release results indicate that micelles do not impede the release of ACV in biorelevant media but slightly improved the release rate, probably by enhancing the penetration of ACV through the dialysis bag.

5.5. *Partition coefficient*

The partition coefficient quantifies the drug's distribution between two phases: the polar phase, typically water, and the non-polar phase, n-octanol. n-Octanol is traditionally used in partition coefficient studies

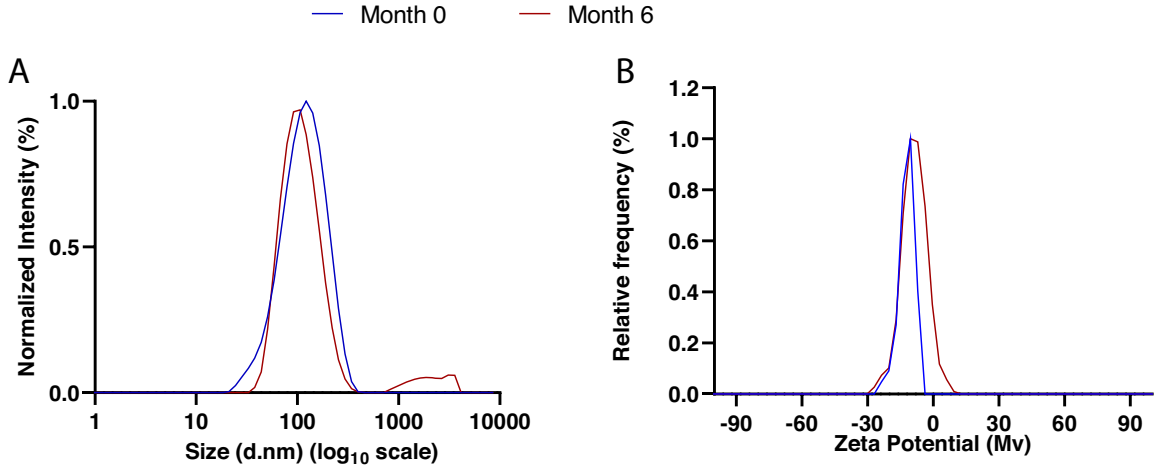

Fig. 5. (A) Hydrodynamic size distribution by intensity of ACV micelles on day 1 (Month 0) and after 6 months, storage at room temperature. (B) Zeta potential of ACV micelles on day 1 (Month 0) and after 6 months, storage at room temperature.

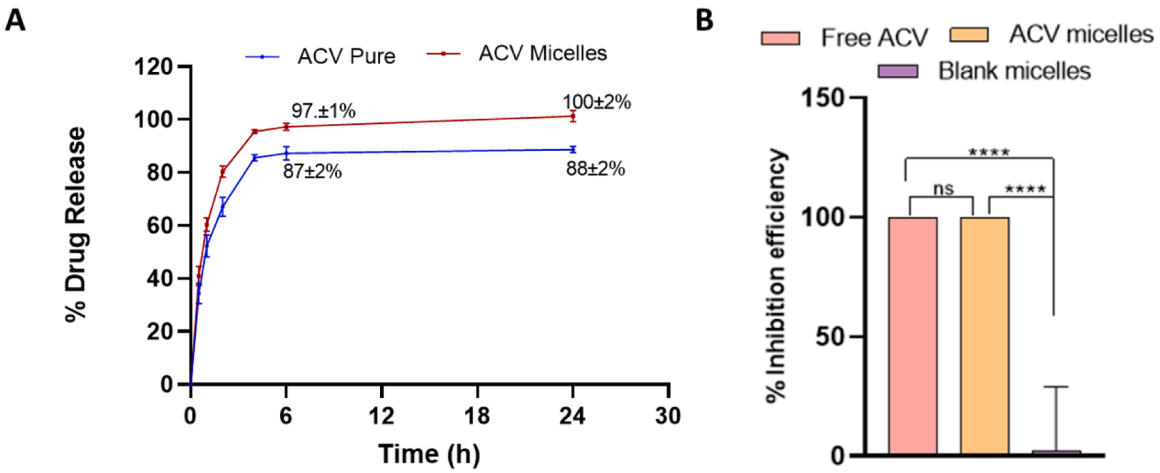

Fig. 6. (A) In vitro ACV release (%) from the polymeric micelles and free ACV (ACV solution in miliQ water), in which sample was first incubated in FaSSGF (pH 1.2) for an initial 2 h and then subsequently in FaSSIF (pH 6.8) buffer at 37 °C ($n = 3$), (B) Plaque reduction assay result. Vero cells were therapeutically treated 2 h post infection and then administered IgG. Plaques were counted 48 h post infection and normalized to untreated (ns=non-significant, *=$P < 0.05$).

because it provides a rough approximation of a compound's lipophilicity and its potential for passive membrane permeability. LogP is a constant value that is negative for compounds that are hydrophilic (they prefer the water phase) and a positive for compounds that are lipophilic (they prefer the lipid/organic solvent phase). Compounds that split evenly between the water and lipid phases are valued at zero. Table 4 displays the logP values for the free ACV and ACV micelles. According to partition coefficient measurement, ACV micelles exhibited a superior lipophilic nature in contrast to free ACV. This difference in logP value indicates that the micelles may enhance the lipophilicity of ACV, potentially improving its absorption and ultimately the bioavailability of ACV micelles (Mandeep et al., 2020).

5.6. Antiviral assay

To ensure that the antiviral efficacy of ACV has not been compromised when formulated into micelles, a series of antiviral assays were carried out and noninferiority was assessed. MG cells, representing neuronal cells, were treated and infected with HSV-1-GFP, and supernatant was quantified for released viruses. The cells were treated both prophylactically (pre-infection) and therapeutically (post-infection) and the treatment was either washed or left in the well. Prophylactic setting was performed to reflect prophylactic dosing in immunocompromised patient groups. Therapeutic setting shows whether the treatment can inhibit viral replication in already infected cells. Washing was performed as there was suspicion that the micelles interfere with the virus in the supernatant and affect the results.

Both the free ACV and ACV micelles did not differ significantly in antiviral efficacy in the prophylactic unwashed setting (Fig. 6). The ACV micelles had increased efficacy in the washed prophylactic setting compared to free ACV ($P = 0.029$, Fig. 7). Both treatments were more efficacious than the corresponding blank micelle treatment ($P = 0.029$). Free ACV and ACV micelles did not differ significantly in both the washed and unwashed therapeutic settings. Blank micelles also showed antiviral activity compared to untreated control in both settings ($P = 0.029$), but drug was more efficacious than the blank control treatment in both settings ($P = 0.029$).

Since the blank micelles also showed antiviral activity in tested conditions it became difficult to conclude that the ACV micelles are equivalently active relevant to free ACV. Consequently, a plaque reduction experiment was designed to evaluate whether antiviral efficacy is due to interference of extracellular virions. By infecting cells prior to treatment, the micelles should not interfere with viral entry, so a therapeutic setting was chosen. Further, the cells were treated with IgG after infection so that any extracellular virion would be neutralized, rendering cell to cell spread the only viable option for viral spread. In this way we can determine whether micelles interfere with extracellular virions or also interfere with viral replication. The results showed no significant difference between free ACV and ACV in micelles, while the blank micelles had no antiviral efficacy compared to untreated cells (Fig. 6B). Both ACV and ACV in micelles were more antiviral than blank micelles ($P = 0.00$). These results are further supported by the imaged MG cells prior to supernatant collection, where all cells are infected in the blank treated wells (Fig. 8). Thus, it can be concluded that ACV in micelles is equally effective to free ACV in inhibition of HSV virus in vitro.

Table 4
Partition coefficient of ACV and ACV micelles using n-octanol and water at 25 °C.

Samples	Aqueous Phase (mg/mL)	Oil Phase (mg/mL)	$P_{O/w}$	LogP
Free ACV	1.31±0.01	0.03	0.02	−1.60
ACV micelles	2.31±0.01	0.28±0.03	0.12	−0.91

5.7. Permeation study

To make sure that the PVPA is an appropriate model to use for the permeability assessment of the ACV formulation, the integrity of the PVPA barriers was assessed by determining the apparent permeability (P_{app}) of free calcein (CAL) solution and CAL in micelles as well as the electrical resistance (ER) across the barriers at the end of each experiment. Additionally, mucus obtained by hydrated mucins was added on top of the barrier (Mucus-PVPA) to study the behavior of the micelles in the presence of a simulated intestinal mucus layer. The ER values were within the accepted limits (290 −1000 Ohm · cm^2) and the results from the permeation of free CAL and CAL from micelles across the PVPA barriers did not show any sign of compromised integrity in all the tested conditions, thus proving that the micelle formulation did not affect the integrity of the PVPA barriers (Fig. 9A).

The permeability of free ACV in solution or ACV in micelles across the PVPA barriers in absence (naked- PVPA) or presence (mucus-PVPA) of mucus were then assessed. As shown in Fig. 9B, and Table 5, the permeation of ACV from the micellar formulation across the PVPA resulted in an apparent permeability (P_{app}) of 0.050 10^{-6} cm/s in absence of mucus and 0.025 10^{-6} cm/s in the presence of mucus, which represents a significantly improved permeability compared to the

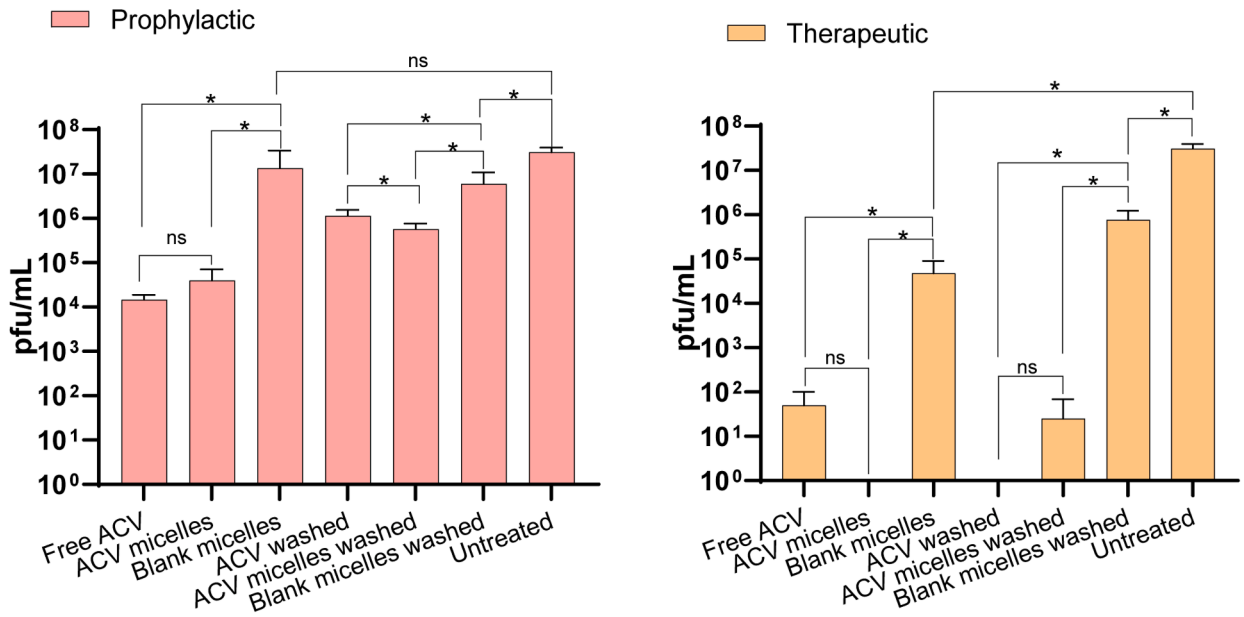

Fig. 7. (A) Titers of the released viruses from the antiviral assay in MG cells. Cells were treated 24 h prophylactically and were either left unwashed or washed 3 h after drug treatment. In another setting the cells were treated 2 h post infection and were either left unwashed or washed 3 h after drug treatment. The shed viruses were collected 48 h after infection and quantified using plaque titration and presented in logarithmic scale as plaque forming units (pfu/mL).

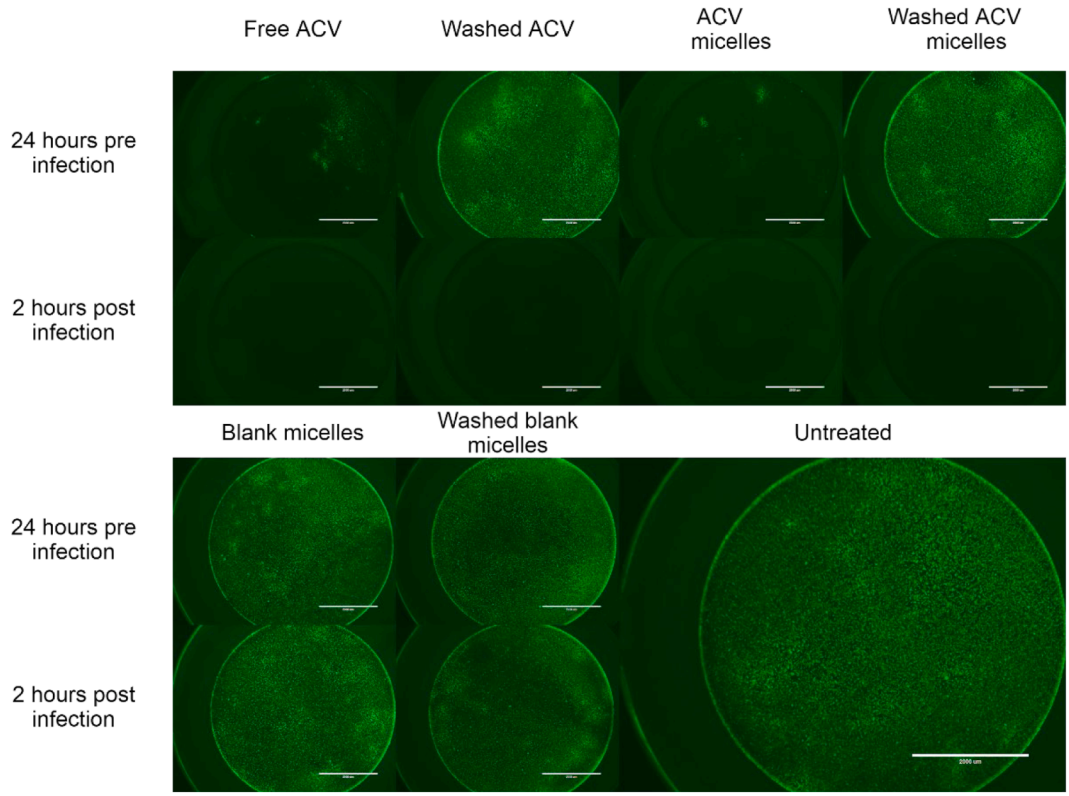

Fig. 8. Representative images of MG cells imaged using EVOS live fluorescence FL 48 h post infection. HSV-1-GFP contains a GFP cassette that is expressed during infection; thus, the degree of green fluorescence reflects the infected cells.

situation with only the free ACV. The amount of free ACV in solution that permeated across the PVPA was below the detection limit of the HPLC method. Therefore, due to the steric and interface barrier properties of mucus, which can further hinder permeation (Boegh et al., 2013), the permeability of free ACV solution across the mucus-PVPA was not tested. Some of the permeation enhancing effects of the micellar formulation were also observed for CAL in micelles, and this further strengthens the hypothesis on an enhanced permeation of drug/compound when carried by the micelles both in the absence and presence of mucus. Similar formulation effects on the permeability of ACV through the PVPA have also earlier been observed when liposomes were used as a carrier for ACV (Naderkhani et al., 2014).

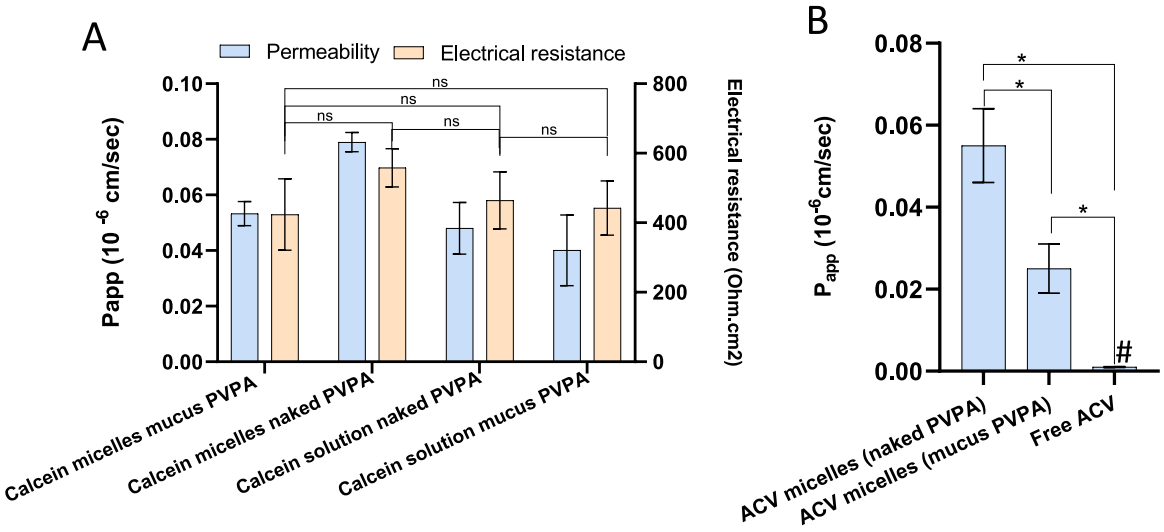

Fig. 9. (A) Calcein apparent permeability (P_{app}) across the PVPA barrier in the absence and presence of mucus (mucus-PVPA) and electrical resistance (ER) values at the end of the experiment; (Mean ± SD; $n = 3$). (B) ACV (Mean ± SD; $n = 6$) apparent permeability (P_{app}) across the PVPA barrier in the absence (naked PVPA) and presence of mucus (mucus PVPA). # The amount of ACV present in the acceptor in the experiment with free ACV was below the detection limit (0.35 μg/mL).

Table 5
ACV and CAL permeability (P_{app}) across the different PVPA barriers/set ups (Mean ± SD; n = 6).

Type of barriers	**Donor solution (Calcein concentration)**	**P_{app} (10^{-6} cm/s)**
Naked Barriers	CAL solution (15 mM)	0.05 ± 0.01
	CAL micelles (10.84 mM)	0.08 ± 0.01
	Free ACV solution	Below detection limit
	ACV micelles	0.05 ± 0.01
Mucus covered barriers	CAL solution (15 mM)	0.04 ± 0.01
	CAL micelles (10.84 mM)	0.06 ± 0.01
	ACV solution	-
	ACV micelles	0.03 ± 0.01

5.8. Cytotoxicity study

The cytotoxicity of the blank micelles was determined by the MTT assay to estimate the safety profile of the PJL based polymeric micelles. Cell viability in MG and MDA-MB-231 cells were established after treatment with mPEG-b-PJL-COOH and B-COOH blank micelles at different concentrations (250, 500 and 750 μg/mL) for 48 h. We have chosen two types of cells (MG and MDA-MB 231) to establish the polymer's cytotoxicity. We used MG cells as they represent neuronal tissue, which is important in the tropism of HSV, and MDA-MB 321 cells as they are known for their proliferative capability. Using both cell lines will provide a comprehensive understanding of the polymer's effects on different types of cells, which will be crucial for evaluating its potential as a therapeutic agent. Fig. 10 shows that both the polymers are well tolerated up to the concentration of 500 μg/mL and demonstrate the

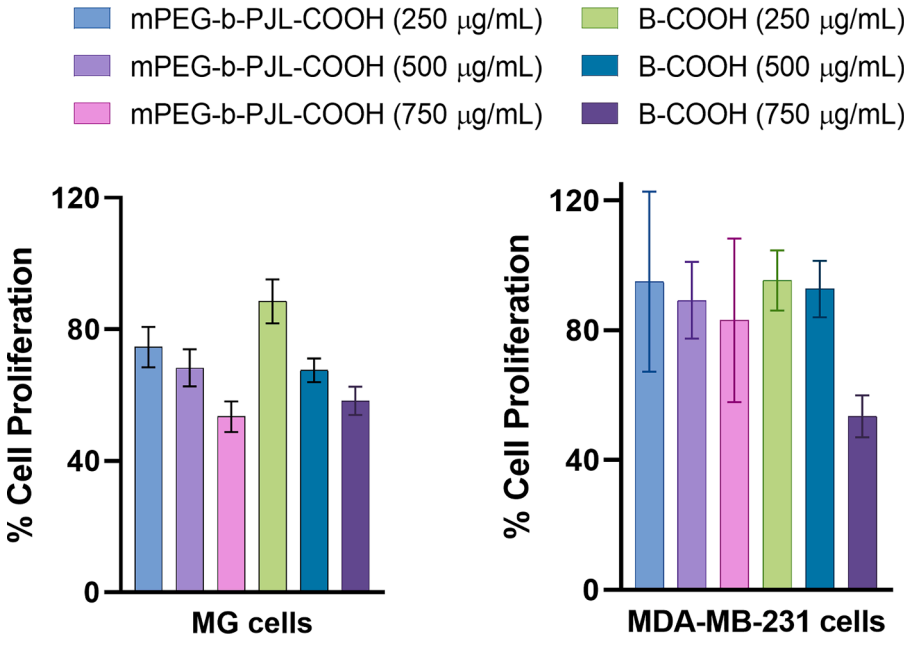

Fig. 10. Cytotoxicity study of polymeric micelles on MG cells and MDA-MB-231 cells based on MTT assay.

signs of toxicity at the concentration of 750 μg/mL, which suggested concentration dependent cytotoxicity profile in both cell lines. B-COOH micelles are slightly more toxic on (up to 40 % cell death) MDA-MB-231 cells compared to mPEG-b-PJL-COOH micelles. Notably, all our antiviral studies were conducted at concentrations below the cytotoxic threshold of the polymeric micelles. Therefore, the cytotoxic effects observed at higher concentrations did not influence the outcomes of antiviral assays.

5.9. GastroPlus based in silico prediction of plasma concentration-time profiles

The GastroPlus program software is a mechanical simulation and prediction tool for pharmacokinetics (PK) and pharmacodynamics (PD) parameters for drugs or formulations and is an extensively used tool for drug development. It was utilized to predict the in vivo plasma drug concentration of ACV micelles and free ACV solution in water. The software uses an advanced compartmental absorption and transit (ACAT) model to simulate and predict the absorption of pure ACV and ACV micelles by the oral route in nine different parts of the gastrointestinal tract (GIT). The "regional absorption compartment model" refers to a series of nine compartments, starting with the stomach followed by the duodenum, jejunum (three), ileum (three), and ascending colon. The GastroPlus software considers that factors such as particle size, composition, physiological condition (intestine, stomach, and duodenum), pH for reference solubility, and apparent permeability could influence the drug's effectiveness. Data shown in Fig. 11(A) displays the anticipated plasma concentration-time profiles of both formulations. The in-silico model predicts that the peak plasma concentration (C_{max}) for ACV micelles could be much higher (approx. 916 ng/mL) than the free ACV solution in water (approx. 426 ng/mL) indicating higher bioavailability of ACV micelles compared to the free ACV. This could be due to enhanced solubility and/or higher permeability of ACV in micelles owing to its small size and negative charge. Moreover, Fig. 11(B) indicates absence of absorption in the gastric region (stomach), whereas the peak absorption of free ACV and ACV micelles occurred in the jejunum1 and jejunum2, followed by the duodenum, while the absorption is minimal beyond these three segments. A similar pattern was seen in previous research, demonstrating that the duodenum in Pept1 knockout mice only absorbed 4 % of the valacyclovir dose, while the jejunal segments and ileum contributed 14 % and 10 %, respectively (Yang and Smith, 2017).

6. Conclusions

In this study, we reported the utilization of polymeric micelles for the first time for improving the aqueous solubility and oral permeability of ACV by utilizing a mixture of mPEG-b-PJL-COOH and B-PJL-COOH polymers. We observed that mixing a small amount of homopolymer B-PJL-COOH during micelle preparation not only improves the drug loading but also enhances the stability of the micelles. The ACV micelles demonstrate 100 % drug release, higher partition coefficient without compromising the in vitro antiviral efficacy of ACV against HSV-1. In vitro permeation tests indicated an improved intestinal permeability of ACV when administered as micelles, in contrast to free ACV, a finding that was later verified by in silico pharmacokinetic modelling predictions. Cytotoxicity assessments demonstrated concentration and cell dependent toxicity, where the concentrations used in antiviral studies were found to be non-toxic. Overall, these findings suggest that ACV micelles offer a viable nanocarrier system for enhancing the stability, bioavailability, and aqueous solubility of ACV and advocate further investigation to establish poly(jasmine lactone) based micelles as nanocarrier for effective delivery of BCS class III drugs.

Funding

This research was partly funded by Business Finland Research-to-Business project Jasmine PRO (1609/31/2021). J.V. acknowledges the funding support provided by National Overseas Scholarship, Ministry of Social Justice and Empowerment, Government of India, for her personal PhD scholarship, and the Swedish Cultural Foundation in Finland for a personal PhD grant (#199,427) and funding from NordForsk for the Nordic University Hub project #85,352 (Nordic POP, Patient Oriented Products) for providing the research mobility to perform the in vitro permeation study at UiT, The Arctic University of Norway, Tromsø, Norway. F.F. would further like to thank Åbo Akademi University Graduate School for personal funding in the form of PhD salary.

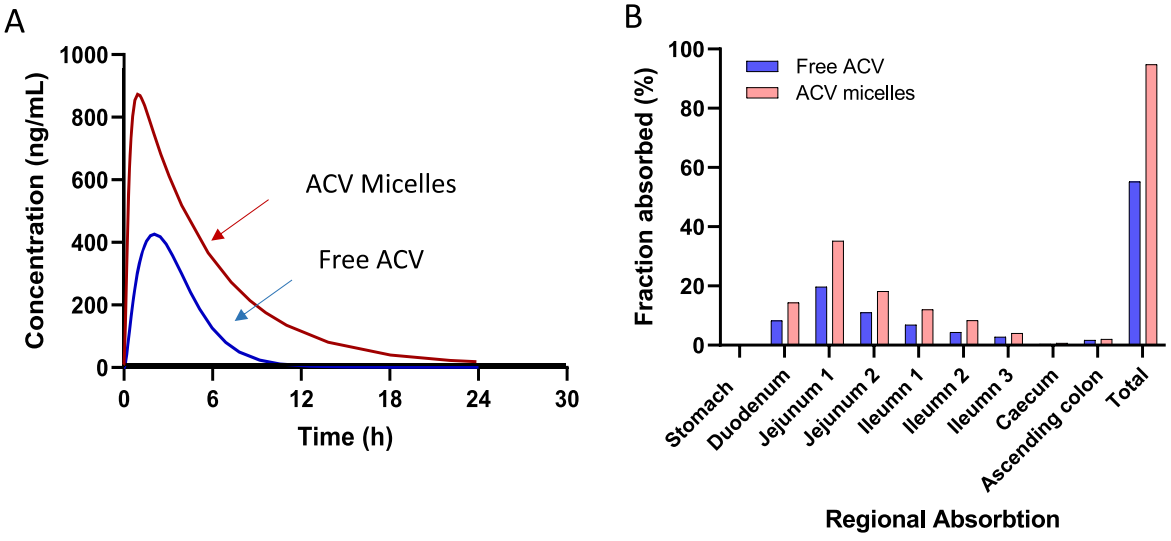

Fig. 11. Predicting data: (A) plasma-drug concentration profile of 100 mg of free ACV (solution) and ACV micelles. These data were obtained from Gastroplus® software (version 10x, SimulationPlus Inc., Lancaster, CA, USA) and (B) the regional absorption.

Declaration of generative AI and AI-assisted technologies in the writing process

During the preparation of this work the author(s) used "quillbot" in order to improve the readability and grammar of the text. After using this service, the author(s) reviewed and edited the content as needed and take(s) full responsibility for the content of the publication.

CRediT authorship contribution statement

Jyoti Verma: Writing – original draft, Methodology, Investigation, Formal analysis. **Fanny Frejborg:** Writing – original draft, Methodology, Investigation, Formal analysis. **Marta Mantegna:** Writing – original draft, Methodology, Investigation, Formal analysis. **Vishal Kumar:** Writing – original draft, Methodology, Investigation, Formal analysis. **Veijo Hukkanen:** Writing – review & editing, Supervision. **Gøril Eide Flaten:** Writing – review & editing, Supervision, Resources, Funding acquisition. **Jessica M. Rosenholm:** Writing – review & editing, Supervision, Resources, Funding acquisition. **Kuldeep K. Bansal:** Writing – review & editing, Supervision, Project administration, Investigation, Conceptualization.

Declaration of competing interest

The authors declare no conflict of interest.

Acknowledgement

The authors would like to acknowledge Lisa Myrseth Hemmingsen, UiT The Arctic University of Norway, for performing HPLC analysis throughout the permeability study of the project. This study is part of the activities of Åbo Akademi Foundation (SÅA) funded Centre of Excellence in Research "Materials-driven solutions for combating antimicrobial resistance (MADNESS)". The activities are also aligned with the strategic research profiling area "Solutions for Health" at Åbo Akademi University [Academy of Finland, # 336355]. We also thank the Jane and Aatos Erkko Foundation for financial support (grant number #170046).

Data availability

Data will be made available on request.

References

Ali, A., Bhadane, R., Asl, A.A., Wilén, C.-E., Salo-Ahen, O., Rosenholm, J.M., Bansal, K.K., 2022. Functional block copolymer micelles based on poly (jasmine lactone) for improving the loading efficiency of weakly basic drugs. RSC Adv. 12, 26763–26775.

Assiri, A.A., Glover, K., Mishra, D., Waite, D., Vora, L.K., Thakur, R.R.S., 2024. Block copolymer micelles as ocular drug delivery systems. Drug Discov. Today 29, 104098.

Ates, M., Kaynak, M.S., Sahin, S., 2016. Effect of permeability enhancers on paracellular permeability of acyclovir. J. Pharm. Pharmacol. 68, 781–790.

Bansal, K.K., A., A.A, Mijanur, R., Erica, S., Carl-Eric, W., Rosenholm, J.M., 2023a. Evaluation of solubilizing potential of functional poly(jasmine lactone) micelles for hydrophobic drugs: a comparison with commercially available polymers. Int. J. Polym. Mater. Polym. Biomater. 72, 1272–1280.

Bansal, K.K., Gupta, J., Rosling, A., Rosenholm, J.M., 2018. Renewable poly (δ-decalactone) based block copolymer micelles as drug delivery vehicle: in vitro and in vivo evaluation. Saudi. Pharm. J. 26, 358–368.

Bansal, K.K., Lariya, N., 2018. Block copolymer micelles in drug delivery and cancer therapy. Chronic Pharm. Sci. 2, 534–544.

Bansal, K.K., Wilen, C.-E., Rosenholm, J.M., 2023b. Synthetic polymers in translational nanomedicine: from concept to prospective products. Curr. Pharm. Des. 29, 2277–2280.

Bansal, K.K., Özliseli, E., Rosling, A., Rosenholm, J.M., 2021. Synthesis and evaluation of novel functional polymers derived from renewable jasmine lactone for stimuli-responsive drug delivery. Adv. Funct. Mater. 31, 2101998.

Boegh, M., Foged, C., Müllertz, A., Nielsen, H.M., 2013. Mucosal drug delivery: barriers, in vitro models and formulation strategies. J. Drug Deliv. Sci. Technol. 23, 383–391.

Bruni, G., Maietta, M., Maggi, L., Ferrara, C., Berbenni, V., Milanese, C., Girella, A., Marini, A., 2013. Preparation and physicochemical characterization of acyclovir cocrystals with improved dissolution properties. J. Pharm. Sci. 102.

Cabral, H., Kataoka, K., 2014. Progress of drug-loaded polymeric micelles into clinical studies. J. Control Release 190, 465–476.

Falavigna, M., Klitgaard, M., Brase, C., Ternullo, S., Škalko-Basnet, N., Flaten, G.E., 2018. Mucus-PVPA (mucus Phospholipid Vesicle-based Permeation Assay): an artificial permeability tool for drug screening and formulation development. Int. J. Pharm. 537, 213–222.

Falavigna, M., Klitgaard, M., Steene, E., Flaten, G.E., 2019. Mimicking regional and fasted/fed state conditions in the intestine with the mucus-PVPA in vitro model: the impact of pH and simulated intestinal fluids on drug permeability. Eur. J. Pharm. Sci. 132, 44–54.

Flaten, G.E., Dhanikula, A.B., Luthman, K., Brandl, M., 2006. Drug permeability across a phospholipid vesicle based barrier: a novel approach for studying passive diffusion. Eur. J. Pharm. Sci. 27, 80–90.

Ghosh, P.K., Majithiya, R.J., Umrethia, M.L., Murthy, R.S.R., 2017. Design and development of microemulsion drug delivery system of acyclovir for improvement of oral bioavailability. AAPS PharmSciTech. 7, 77.

Gnann Jr., J.W., Barton, N.H., Whitley, R.J., 1983. Acyclovir: mechanism of action, pharmacokinetics, safety and clinical applications. Pharmacotherapy. 3, 275–283.

Kalke, K., Orpana, J., Lasanen, T., Esparta, O., Lund, L.M., Frejborg, F., Vuorinen, T., Paavilainen, H., Hukkanen, V., 2022. The In vitro replication, spread, and oncolytic potential of Finnish circulating strains of herpes simplex virus type 1. Viruses 14.

Kasif, M., Gupta, R., Singh, P.P., Bhardwaj, P., Goyal, R., Bansal, K.K., Mahor, A.K., 2024. Development of biocompatible lipid-polymer hybrid nanoparticles for enhanced oral absorption of posaconazole: a mechanistic in vitro and in silico assessment. J. Drug Deliv. Sci. Technol. 101, 106109.

Kedar, U., Phutane, P., Shidhaye, S., Kadam, V., 2010. Advances in polymeric micelles for drug delivery and tumor targeting. Nanomed. Nanotechnol. Biol Med. 6, 714–729.

Lamson, N.G., Berger, A., Fein, K.C., Whitehead, K.A., 2020. Anionic nanoparticles enable the oral delivery of proteins by enhancing intestinal permeability. Nat. Biomed. Eng. 4, 84–96.

Lee, B., Moon, K.M., Kim, C.Y., 2018. Tight junction in the intestinal epithelium: its association with diseases and regulation by phytochemicals. J. Immunol. Res. 2018, 2645465.

Mandeep, Kaur, S., Samal, S.K., Roy, S., Sangamwar, A.T., 2020. Successful oral delivery of fexofenadine hydrochloride by improving permeability via phospholipid complexation. Eur. J. Pharm. Sci. 149, 105338.

Naderkhani, E., Isaksson, J., Ryzhakov, A., Flaten, G.E., 2014. Development of a Biomimetic Phospholipid Vesicle-based Permeation Assay for the Estimation of Intestinal Drug Permeability. Journal of Pharmaceutical Sciences 103, 1882–1890.

Naderkhani, E., Vasskog, T., Flaten, G.E., 2015. Biomimetic PVPA in vitro model for estimation of the intestinal drug permeability using fasted and fed state simulated intestinal fluids. Eur. J. Pharm. Sci. 73, 64–71.

Nair, A.B., Attimarad, M., Al-Dhubiab, B.E., Wadhwa, J., Harsha, S., Ahmed, M., 2014. Enhanced oral bioavailability of acyclovir by inclusion complex using hydroxypropyl-β-cyclodextrin. Drug Deliv. 21, 540–547.

Pyrhönen, J., Bansal, K.K., Bhadane, R., Wilén, C.-E., Salo-Ahen, O.M.H., Rosenholm, J. M., 2022. Molecular dynamics prediction verified by experimental evaluation of the solubility of different drugs in poly(decalactone) for the fabrication of polymeric nanoemulsions. Adv. Nanobiomed. Res. 2, 2100072.

Rahman, M., Ali, A., Sjöholm, E., Soindinsalo, S., Wilén, C.-E., Bansal, K.K., Rosenholm, J.M., 2022. Significance of polymers with "Allyl" functionality in biomedicine: an emerging class of functional polymers. Pharmaceutics. 14, 798.

Saifi, Z., Rizwanullah, M., Mir, S.R., Amin, S., 2020. Bilosomes nanocarriers for improved oral bioavailability of acyclovir: a complete characterization through in vitro, ex-vivo and in vivo assessment. J. Drug Deliv. Sci. Technol. 57, 101634.

Salimi, A., Sharif Makhmal Zadeh, B., Kazemi, M., 2019. Preparation and optimization of polymeric micelles as an oral drug delivery system for deferoxamine mesylate: in vitro and ex vivo studies. Res. Pharm. Sci. 14, 293–307.

Shakri, A., Mohd Paad, K., Saad, N., Mohamed Suffian, I.F., 2025. Gemcitabine-loaded poly (lactide-co-glycolide) – poly (ethylene glycol) gold nanoparticles: evaluating the effect of fabricating methods on physicochemical characteristics, in vitro drug release and cytotoxicity. Drug Deliv. Transl. Res.

Shamshina, J.L., Cojocaru, O.A., Kelley, S.P., Bica, K., Wallace, S.P., Gurau, G., Rogers, R. D., 2017. Acyclovir as an ionic liquid cation or anion can improve aqueous solubility. ACS. Omega 2, 3483–3493.

Sköldenberg, B., Forsgren, M., Alestig, K., Bergström, T., Burman, L., Dahlqvist, E., Forkman, A., Frydén, A., Lövgren, K., Norlin, K., et al., 1984. Acyclovir versus vidarabine in herpes simplex encephalitis. Randomised multicentre study in consecutive Swedish patients. Lancet 2, 707–711.

Snijder, B., Sacher, R., Rämö, P., Liberali, P., Mench, K., Wolfrum, N., Burleigh, L., Scott, C.C., Verheije, M.H., Mercer, J., Moese, S., Heger, T., Theusner, K., Jurgeit, A., Lamparter, D., Balistreri, G., Schelhaas, M., De Haan, C.A.M., Marjomäki, V., Hyypiä, T., Rottier, P.J.M., Sodeik, B., Marsh, M., Gruenberg, J., Amara, A., Greber, U., Helenius, A., Pelkmans, L., 2012. Single-cell analysis of population context advances RNAi screening at multiple levels. Mol. Syst. Biol. 8, 579.

Spleis, H., Sandmeier, M., Claus, V., Bernkop-Schnürch, A., 2023. Surface design of nanocarriers: key to more efficient oral drug delivery systems. Adv. Colloid. Interface Sci. 313, 102848.

Sze, L.P., Li, H.Y., Lai, K.L.A., Chow, S.F., Li, Q., KennethTo, K.W., Lam, T.N.T., Lee, W.Y. T., 2019. Oral delivery of paclitaxel by polymeric micelles: a comparison of different block length on uptake, permeability and oral bioavailability. Colloids. Surf. B Biointerfaces 184, 110554.

Xie, B., Liu, Y., Li, X., Yang, P., He, W., 2024. Solubilization techniques used for poorly water-soluble drugs. Acta Pharm. Sin. B 14, 4683–4716.

Yan, Y., Chen, J.-M., Lu, T.-B., 2013. Simultaneously enhancing the solubility and permeability of acyclovir by crystal engineering approach. Cryst. Eng. Comm. 15, 6457–6460.

Yang, B., Smith, D.E., 2017. In Silico absorption analysis of valacyclovir in wildtype and Pept1 knockout mice following oral dose escalation. Pharm. Res. 34, 2349–2361.

Yu, Z., Fan, W., Wang, L., Qi, J., Lu, Y., Wu, W., 2019. Effect of surface charges on oral absorption of intact solid lipid nanoparticles. Mol. Pharm. 16, 5013–5024.